Published in final edited form as:
J Immunol. 2010 June 1; 184(11): 6256–6265. doi:10.4049/jimmunol.0901463.

Identification and characterisation of a lupus suppressor 129 locus on chromosome 3[1]

Francesco Carlucci[*], **Liliane Fossati-Jimack**[*], **Ingrid E. Dumitriu**[*], **Yasin Heidari**[*], **Mark J. Walport**[*,2], **Marta Szajna**[*], **Paramita Baruah**[*], **Oliver A. Garden**[‡], **H. Terence Cook**[†], and **Marina Botto**[*,3]

[*]Rheumatology Section, Faculty of Medicine, Imperial College, Hammersmith Campus, London, UK

[†]Department of Histopathology, Faculty of Medicine, Imperial College, Hammersmith Campus, London, UK

[‡]Department of Veterinary Clinical Sciences, The Royal Veterinary College, London, UK

Abstract

The 129-derived *Sle16* is a susceptibility locus for systemic autoimmunity when present on the C57BL/6 (B6) background. Genetic analysis of a (129×B6)F2 cross identified a region from the B6 chromosome 3 (*Sle18*) with positive linkage to anti-nuclear antibodies. Here we have generated a B6 congenic strain harbouring the 129 allele of *Sle18* and intercrossed this line with the lupus-prone B6.129-*Sle16* strain. The presence of the 129-*Sle18* allele in the B6.129-*Sle16Sle18* double congenic mice suppressed the development of *Sle16*-mediated autoantibody production and ameliorated the renal pathology. The 129-*Sle18* locus rectified the B cell abnormalities detected in the B6.129-*Sle16* mice, such as the reduction in the percentage of marginal zone B and B1a cells and the increased number of germinal centers. The B6.129-*Sle16Sle18* spleens still displayed an increased percentage of activated T and B cells. However, in the B6.129-*Sle16Sle18* strain the percentage of naïve T cells was equivalent to that in B6.129-*Sle18* and B6 mice and these cells showed a reduced proliferative response to anti-CD3 stimulation compared to B6.129-*Sle16* T cells. There was a significant increase in the percentage of $CD4^+FoxP3^+$regulatory T cells in all congenic strains. These cells had normal regulatory function when tested *in vitro*. Thus 129-*Sle18* represents a novel, non-MHC lupus-suppressor locus probably operating as a functional modifier of B cells that, in combination with other factors, leads to lupus resistance. Further characterisation of this locus will help to uncover the immune mechanism(s) conferring protection against lupus.

Keywords

systemic lupus erythematosus; autoantibodies; rodent; congenic

[1]This work was supported by the Wellcome Trust (grant number 071467).

Correspondence address: Marina Botto Rheumatology Section, Faculty of Medicine Imperial College, Hammersmith Campus Du Cane Road, London W12 0NN, UK Tel.: +44-(0)20 8383 2316 Fax: +44-(0)20 8383 2379 m.botto@imperial.ac.uk. [3]Correspondence address**:** Rheumatology Section, Faculty of Medicine Imperial College, Hammersmith Campus Du Cane Road, London W12 0NN, UK Tel.: +44-(0)208-383 2316 Fax: +44-(0)208-743 3109 m.botto@imperial.ac.uk.
[2]Current address: The Wellcome Trust, London, UK

Europe PMC Funders Author Manuscripts

Introduction

The spontaneous occurrence of autoimmunity is the product of genetic, environmental and stochastic events most likely occurring concurrently. In the autoimmune disorder Systemic Lupus Erythematosus (SLE), numerous disease susceptibility loci have been identified both in human and animal studies (1, 2). Findings from lupus-prone mice and congenic lines have proved that genetic predisposition to SLE is caused by epistatic interactions between several genes spread throughout the genome and organised in susceptibility and modifier/suppressor loci (3). These genes may regulate different pathogenic aspects of SLE, influence the severity of the clinical manifestations and affect the outcome of the disease.

Congenic mouse models have facilitated the dissection of the intricate pathogenic pathways leading to SLE. The genetic analysis of these strains remains a strategy of great value especially for the identification of loci, and the genes within, with a “suppressive” role that are still perhaps beyond the feasibility of the current genome wide association studies performed on SLE patients. Extensive analysis of the genetic and immunological traits in the B6.NZM2410 collection of congenic sub-strains has demonstrated that the severe lupus-like disease developed by the NZM2410 parental strain is the result of a complex epistatic interaction amongst the individual phenotypes driven by each susceptibility allele (4). Of note, when two potent NZW loci *Sle1* and *Sle3* were combined on the C57BL/6 (B6) background (bi-congenic strain), a lethal autoimmune phenotype resulted. This feature was absent in the NZW strain, suggesting the existence of other chromosomal regions in the parental genome, distinct from the susceptibility loci, capable of suppressing the spontaneous development of autoimmunity. These genomic regions have been defined and named SLE suppressor loci (3, 5).

We have previously presented the results of an extensive linkage trait analysis in the (B6 × 129) hybrid strain that unveiled four main susceptibility loci linked to autoimmune traits (6, 7). The most powerful locus, called *Sle16*, is a 7.4 Mb 129 interval on chromosome 1, which overlaps with many other SLE susceptibility loci both in humans and animal models (8). This locus is capable of driving the production of high levels of autoantibodies and the development of mild glomerulonephritis when transferred on a B6 background, as observed in the B6.129-*Sle16* congenic strain previously named B6.129chr1b. However, the lack of a comparable autoimmune phenotype in the 129 strain indicates that the same strain contains modifier loci, most likely outside the chromosome 1 fragment, with protective effect(s). Likewise, the data imply that the B6 strain is permissive to the development of autoimmunity, also suggested by the observation that a large number of genetically modified models present an obvious disease only on a B6 background (9). Consistent with these hypotheses, linkage analysis performed on the (B6 × 129) hybrid strain identified a B6 lupus locus on chromosome 3, termed *Sle18*, contributing to anti-nuclear (ANA) antibody production. Experiments from our group have recently established that the B6 *Sle18* fragment when transferred onto a 129 background, the 129.B6-*Sle18* congenic model, can promote autoantibody production, increase T and B cell activation, and mediate mild glomerulonephritis (10). To further demonstrate that B6 *Sle18* locus is a key lupus modifier that in epistatic interaction with *Sle16* allows the development of autoantibodies in the B6.129-*Sle16* congenic mice, we adopted a reciprocal approach and transferred the protective 129 region onto the B6 strain. This novel congenic strain, named B6.129-*Sle18,* was then crossed with the B6.129-*Sle16* line and the serological and cellular features of the bi-congenic mice, B6.129-*Sle16Sle18*, were compared with the two single congenic strains and the B6 controls. As predicted by genetic analysis, the presence of the 129 allele at the *Sle18* locus significantly modified the autoantibody profile of the B6.129-*Sle16* mice. However, even though the B6.129-*Sle16Sle18* bi-congenic mice developed markedly less serological features of autoimmunity, signs of splenic B and T cell activation similar to

those described in the B6.129-*Sle16* autoimmune mice were still detectable, indicating that the *Sle18* suppressor locus acted downstream of these molecular pathways. In keeping with this observation, the number of splenic germinal centers in the B6.129-*Sle16Sle18* mice was significantly reduced. Taken together, these data emphasize further the polygenic nature of the aetiology and pathogenesis of SLE.

Materials and Methods

Mice

The generation of B6.129-*Sle16* mice has been previously described (8). A new B6 congenic line, carrying a chromosome 3 interval of 129 origin (*Sle18*), was generated using microsatellite markers polymorphic between 129 and B6 mice as previously described (6, 7, 10). After 8 generations of backcrosses, over 99% of the genome in these mice was of B6 origin and a congenic line (referred to as B6.129–*Sle18)* was created. At the end of the backcrossing, additional microsatellite analyses were carried out in the congenic mice to exclude the presence of unselected 129 genomic regions. The B6.129-*Sle16Sle18* bi-congenic line was then derived by a B6.129-*Sle16* x B6.129-*Sle18* cross (Figure 1). Only female and homozygous mice entered the study. Twenty-eight B6.129-*Sle16*, 29 B6.129-*Sle16Sle18*, 26 B6.129-*Sle18* mice along with 25 sex-matched B6 controls were followed up to one year of age, when all mice were sacrificed and organs collected. Animals were kept under specific pathogen-free conditions and all animal care and procedures were conducted according to institutional guidelines.

Serology

All mice were bled at regular intervals starting from 4 months of age and the assays described below were conducted on serum samples:

- **i.** Titres of IgG ANA were measured by indirect immunofluorescence using Hep-2 cells as previously illustrated (8).
- **ii.** Anti-ssDNA, anti-dsDNA and anti-chromatin antibodies were detected by capture ELISA. The results were expressed in arbitrary ELISA units (AEU) relative to a standard positive sample derived from a serum pool from MRL/Mp.*lpr/lpr* mice (8).
- **iii.** For the detection of anti-histone antibodies by ELISA, microtiter plates were coated with histone (Roche, Hertfordshire, UK) at 5 μg/ml. Samples were screened at 1/500 dilution, bound antibodies were detected with AP-conjugated goat anti-mouse IgG (γ-chain specific) (Sigma-Aldrich, Dorset, UK) and the results were presented in AEU relative to a standard positive sample derived from a serum pool from MRL/Mp.*lpr/lpr* mice.

Renal assessment

Overnight urine specimens were collected from one year-old mice and proteinuria assessed using Haema-combistix (Bayer Diagnostics, Newbury, UK) (8). Kidneys were fixed in Bouin's solution for at least 2 hours, transferred into 70% v/v ethanol, and processed into paraffin. Periodic acid-Schiff stained 3 micron thick sections were scored for glomerulonephritis (GN). Glomerular cellularity was ranked in a blinded fashion as follows: grade 0, normal; grade 1, hypercellularity involving greater than 50% of the glomerular tuft in 25-50% of glomeruli; grade 2, hypercellularity involving greater than 50% of the glomerular tuft in 50%-75% of glomeruli; grade 3, hypercellularity involving greater than 75% of the glomeruli or crescents in greater than 25% of glomeruli; grade 4, severe proliferative glomerulonephritis in greater than the 90% of glomeruli. Additional

morphological characteristics such as crescent formation and peri-glomerular fibrosis were also noted.

Flow cytometry

Cells were harvested from spleens of at least seven mice from each group at two, six and 12 months of age. After depletion of red blood cells (RBCs) using RBC lysis buffer (Tris base plus NH_4Cl), spleen cells were counted and flow cytometry was performed using a three- or four-colour staining protocol and analysed with a FACSCalibur™ (Becton-Dickinson, Mountain View, CA, USA). The following antibodies were used: anti-CD90.2 (53-2.1), anti-B220 (RA3-6B2), anti-CD21 (7G6), anti-CD23 (B3B4), anti-CD138 (281-2), anti-CD5 (53-7.3), anti-CD19 (1D3), anti-CD25 (PC61), anti-CD69 (H1.2F3), anti-CD11b (M1-70), anti-CD11c (HL3), anti-IgM (II/41), anti-CD62L (MEL-14), anti-CD44 (IM7), anti-CD4 (RM4-5), anti-CD8 (53-6.7). All antibodies were purchased from BD Biosciences Pharmingen (San Diego, CA, USA) with the exception of anti-Foxp3 (FJK-16s) (eBioscience, San Diego, CA, USA). Biotinylated antibodies were detected using an allophycocyanin-conjugated streptavidin antibody (BD Biosciences Pharmingen, San Diego, CA, USA). Staining was performed in the presence of a saturating concentration of 2.4G2 monoclonal antibody (anti-FcγRII/III). For the FoxP3 intracellular staining, cells were fixed and lysed with the reagents and the protocol provided by the company (eBioscience, San Diego, CA, USA). Data were analysed using FlowJo software, version 6.4 (TreeStar Inc, Ashland, OR, USA).

Spleen histology

Frozen spleen sections (5μm thick), pre-treated with biotin-blocking system as instructed by the manufacturer (Dako, Glostrup, Denmark), were incubated overnight with biotinylated anti-mouse GL7 diluted 1/50 (eBioscience, San Diego, CA, USA). Streptavidin PE (1/100) (BD Biosciences PharMingen, San Diego, CA) was then applied for 30 minutes and samples were then incubated with 4′,6-diamidino-2-phenylindole (DAPI) (1/1000) (Invitrogen, Carlsbad, CA) for 10 minutes. Three different sections per sample were cut every 100 μm and stained. Quantitative analysis was performed by counting the number of germinal centers, identified by GL7+ cells, and the average was divided by the spleen sectional area at each cutting level. The sectional area was determined by taking images with a Photonic Science Color Coolview digital camera (Photonic Science , East Sussex, UK) and drawing around the profile of the spleen section using the *Image ProPlus*™ software (version 4.5, Media Cybernetics, USA). Further immunohistochemical analysis of spleen sections was performed combining the GL7 staining with a rat anti-mouse FITC-labeled IgD antibody (1/100) (BD Biosciences PharMingen). Slides were viewed using an Olympus BX4 fluorescence microscope (Olympus Optical, London, UK) and images were acquired with a Photonic Science Color Coolview digital camera (Photonic Science, East Sussex, UK).

In vitro B and T cell assays

i) B cell assays—Single cell suspension of splenocytes (10^6 cells/ml) were cultured with either LPS (0.5 and 0.05 μg/ml, Sigma-Aldrich, Dorset, UK) or goat anti-mouse IgM(Fab)′$_2$ (10 and 5 μg/ml, Pierce Biotechnology Inc, Rockford, IL, USA) or rat anti-mouse CD40 (FGK45) (2.5 μg/ml, Alexis Biochemicals, Lausen, Switzerland) ± IL-4 (10ng/ml, R&D Systems, Minneapolis, MN, USA). After 18 hours cells were phenotyped with antibodies to CD19, CD69 and CD86. At different time points (48hours and 72hours) production of IgM and IgG were measured in the supernatants by ELISA. Each assay included at least 3 mice per group and the experiments were repeated 3 times.

Europe PMC Funders Author Manuscripts

ii) T cell assays—Purified T cells were negatively selected from spleens and selected lymph nodes from B6, B6.129-*Sle16*, B6.129-*Sle16Sle18* or 129.B6–*Sle18* mice and then activated with plate-bound anti-CD3 (from 1 to 30ug/ml) or phytohemagglutinin (PHA) (from 1 to 10 ug/ml) for 3 days. Tritiated thymidine (^{3}H-TdR) was added 16hours prior to harvesting and incorporation was measured by liquid scintillation. Each assay was repeated at least three times. A sandwich ELISA for IL-2 was performed using purified capture and biotinylated detection antibodies from BD Biosciences Pharmingen (San Diego, CA, USA).

iii) T cell Suppression assays—This assay was performed as previously reported (11). Negative magnetic selection of $CD4^+$ T cells from spleens and selected lymph nodes was carried out using DynaBeads (Dynal, Oslo, Norway) accordingly to the manufacturer's instructions. $CD4^+CD25^+$ T cells (Treg) were positively selected on MiniMACS columns (Miltenyi, Bergish Gladbach, Germany), using anti-CD25-PE antibodies and anti-PE-MicroBeads (Miltenyi, Bergish Gladbach, Germany). The cell purity was found to be more than 90% as determined by flow cytometry. Purified $CD4^+CD25^+$ T cells were cultured, in 96-well round-bottomed plates, with $CD25^-$ responder T cells (Tresp) in the presence of Epoxy DynaBeads (1 bead/5 cells; Dynal) coated with anti-CD3 and anti-CD28 mAb. $CD4^+CD25^+$ T cells purified from either the B6 or 129.B6-*Sle16* or B6.129-*Sle16Sle18* mice were added to B6 $CD25^-$ T cells at different Treg/Tresp ratios ranging from 1:1 to 1:32. Irradiated $CD25^-$ T cells were used as control. After 3 days the incorporation of ^{3}H-TdR (Amersham Biosciences, Roosendaal, The Netherlands) over 16 hours was measured. In addition, $CD25^-$ T cells were pre-labelled with CFSE (0.5 uM; Molecular Probes, Invitrogen) and cultured in the presence of Epoxy DynaBeads (1 bead/5 cells; Dynal, Invitrogen) coated with anti-CD3 and anti-CD28 mAb either alone or with Treg at different ratios. The Tresp:Treg cocultures were incubated for 96 hours, after which the proliferation of T cells was analysed by flow cytometry. All assays were performed with RPMI 1640 supplemented with 100 units/ml penicillin/streptomycin (GIBCO, Paisley, UK), 2 mM L-glutamine, 10 mM HEPES, and 10% (v/v) heat-inactivated fetal calf serum.

Immunization

The primary immune response to a T-dependent (TD) antigen was assessed following a subcutaneous injection with 50 μg/mouse of 4-hydroxy-3-nitrophenylacetyl conjugated to chicken gamma globulin (NP-CGG) (Biosearch Technologies, Novato CA, USA) in complete Freund's adjuvant (Sigma-Aldrich, Dorset, UK). Sera were tested by ELISA every week for five consecutive weeks after the first immunization. Briefly, plates were coated with 5 μg/ml NP-BSA (Biosearch Technologies Novato CA, USA) and sera were assessed at 1/100 dilution. Bound antibodies were detected with AP-conjugated antibodies to specific mouse isotypes (Southern Biotechnology Associates, Inc., Birmingham, AL). For secondary immunization, mice were boosted with the same dose of NP-CGG in incomplete Freund's adjuvant 28 days after the first injection and antibody titres were measured one week later.

Responses to a T-independent (TI) antigen mice were assessed following intraperitoneal injections with 500μl of Pneumovax II (Sanofi Pasteur MSD Ltd, Berkshire, UK) containing 1μg of each of the 23 main polysaccharides (PS). Serum samples were obtained weekly and the immune response against polysaccharide was measured by ELISA. Microtiter plates were coated with 2 μg/ml of Pneumovax II, sera diluted 1/100 (for IgG3) and 1/1000 (for total IgM) and bound antibodies were detected with AP-conjugated antibodies to specific mouse isotypes (Southern Biotechnology Associates, Inc., Birmingham, AL). Five to seven mice per group were used for each time point.

Statistics

The data are presented as median with respective range of values in parentheses unless otherwise stated. The non-parametric Kruskal-Wallis test with Dunn's multiple comparison test or the Mann-Whitney U-test were applied throughout, with differences being considered significant for p values <0.05. Data from *in vitro* assays were analysed by two-tailed Student's t-test for unpaired samples. Statistics were calculated using GraphPad Prism version 3.0 (GraphPad Software, San Diego, CA).

Results

The 129 allele of Sle18 suppresses autoantibody production driven by Sle16

Our previous work (10) demonstrated the presence of a B6-derived epistatic modifier on chromosome 3 (*Sle18)*, which was permissive for the break in tolerance mediated by *Sle16*. Consequently, the corresponding 129 allele was hypothesised to be a lupus suppressor locus. To test this hypothesis, the central portion of the 129 chromosome 3 was transferred onto the B6 genetic background to create a congenic strain using a marker-assisted selection protocol as described previously. The 129 interval from 71.4Mbp to 129.8Mbp in the B6.129-*Sle18* congenic line was defined as the 129 allele of the *Sle18* locus (Figure 1). Autoimmune traits in B6.129-*Sle18* mice and in B6.129-*Sle16Sle18* bi-congenics were monitored over a one year period and compared with the titres present in B6.129-*Sle16* mice, known to develop high titre of lupus-associated autoantibodies (8).

At 4 months of age the B6.129-*Sle16* mice already displayed high titres of anti-ssDNA IgG Abs compared to the B6 controls (B6.129-*Sle16*: 32.43 AEU, range 3.63-228.9; B6: 4.8 AEU, range 1.6-9.42, p<0.01, Kruskal-Wallis test with Dunn's multiple comparison test). More importantly, the B6.129-*Sle16Sle18* bi-congenic mice had similar titres to those detected in B6 mice and were significantly less autoimmune than the B6.129-*Sle1*6 line (B6.129-*Sle16Sle18*: 12.11 AEU, range 0-188.5, p<0.01 *vs* B6.129-*Sle1*6, Kruskal-Wallis test with Dunn's multiple comparison test). These initial observations were confirmed at all subsequent time points (6, 9 and 12 months). At the one year final time point, when a more extensive study of the autoimmune profile was performed, the B6.129-*Sle16Sle18* bi-congenics still showed autoantibody titres (ANA, anti-dsDNA, anti-ssDNA and anti-histone Abs) equivalent to those measured in B6 mice and statistically lower (p<0.001, Kruskal-Wallis test with Dunn's multiple comparison test) than the values detected in B6.129-*Sle16* animals (Figure 2 A-E). Notably, B6.129-*Sle18* mice had even lower anti-ssDNA and anti-dsDNA Ab values compared to those in B6 controls (B6.129-*Sle18 vs* B6: anti-ssDNA Abs p<0.05; anti-dsDNA Abs p<0.01, Kruskal-Wallis test with Dunn's multiple comparison test) (Figure 2B and 2C). In addition, the analysis of a separate cohort of 6 month-old mice heterozygous at the *Sle18* locus showed anti-ssDNA and anti-chromatin Ab levels significantly lower compared to those present in the B6.129-*Sle16* animals (anti-ssDNA Abs: B6.129-*Sle16* = 80.5 AEU, range 20-3398, n=16 *vs* B6.129-*Sle16Sle18het* = 27 AEU, range 10-320, n=18 p<0.05, Mann Whitney U test; anti-chromatin Abs: B6.129-*Sle16* = 13.2 AEU, range 0-76.94, n=18 *vs* B6.129-*Sle16Sle18het* = 0 AEU, range 0-44.91, n=14 p<0.05, Mann Whitney U test). The anti-dsDNA Ab levels showed the same trend but the difference did not reach statistical significance (B6.129-*Sle16* 8.32 AEU, range 1.3-57.8, n=10 *vs* B6.129-*Sle16Sle18het* 2.18, range 1.5-3.4, n=8, p =????, Mann Whitney U test) . These findings suggest that the presence of a single 129–derived allele on chromosome 3 is sufficient to alter the serological phenotype driven by the *Sle16* locus and indicate that 129-*Sle18* locus may operate in a dominant fashion.

The 129 Sle18 locus ameliorates the renal pathology present in B6.129-Sle16 mice

All mice were sacrificed at 12 months of age and organ and urine collections performed. Kidneys were processed for light microscopy analysis. No signs of abnormal renal function were found in any of the congenic groups or in the control mice (data not shown).

PAS-stained kidney sections were graded in a blinded fashion from 0 to 4 as described in Materials and Methods. As previously reported (8), B6.129-*Sle16* mice developed mild glomerulonephritis (median grade 2, range 0-4), statistically more severe ($p<0.001$, Kruskal-Wallis test with Dunn's multiple comparison test) than B6 mice (median grade 1, range 0-3). In the same analysis, B6.129-*Sle16Sle18* kidney sections presented a glomerulonephritis grade (median grade 1, range 0-4) lower than that of B6.129-*Sle16* mice ($p<0.001$, Kruskal-Wallis test with Dunn's multiple comparison test) and similar to that in wild-type control animals (Figure 2F).

Lupus-resistant and lupus-prone mice display similar splenic changes

To investigate the impact of the 129-*Sle18* locus at the cellular level, we performed a comprehensive flow cytometric analysis of splenocytes from all three (B6.129-*Sle16*, B6.129-*Sle16Sle18*, and B6.129-*Sle18*) congenic lines at 2, 6 and 12 months of age and compared the findings with age-matched B6 controls. As previously reported at 2 months of age, the only splenic alteration detectable was a small but significant decrease in the percentage of marginal zone (MZ) $CD21^{high}CD23^{low}$ B cells in the B6.129-*Sle16* congenics compared to the controls (B6.129-*Sle16*: 4.29 ± 0.4, n=13 vs B6: 6.54 ± 0.54, n=12, $p<0.01$, Mann Whitney test), associated with a parallel trend towards a reduction in the absolute number.

At the 6-month time point, the most striking abnormality was the marked expansion of the percentage of regulatory T cells (Tregs), determined by FoxP3 expression, in all three congenic lines compared to the B6 controls (Table I). This was associated with a significant increase in the absolute number of Tregs only in the B6.129-*Sle16* congenic mice most likely as a result of the tendency of these mice to develop hypercellularity. The expansion of the $FoxP3^+$ T population persisted until the end point (Table I) and was not accompanied by a variation in the intensity of the FoxP3 expression (data not shown). Another interesting finding at 6 months of age was the marked increase in the percentage of activated T cells ($CD69^+$) in the B6.129-*Sle16* and B6.129-*Sle16Sle18* congenic animals. Though this finding was predictable for the lupus-prone strain, the detection of a similar change in the non-autoimmune B6.129-*Sle16Sle18* strain was intriguing and indicated that lupus resistance was not referable to a block in the mechanism controlling T cell activation.

The final analysis performed on samples from 12 month-old mice corroborated the numerous cellular differences between B6.129-*Sle16* and B6 mice already described (8) and provided some novel findings. Splenomegaly was detected only in the lupus-prone B6.129-*Sle16* strain, indicating that 129-*Sle18* maintained normal splenic cellularity. As the B6.129-*Sle16* spleens were markedly hypercellular, only the results expressed as percentages will be discussed, although the absolute numbers reflected these differences in a more exaggerated manner. As expected, the B6.129-*Sle16* mice displayed a more "active" phenotype with a statistically significant increase in activated ($CD69^+$) B and T cells compared to the B6 mice. As observed at the earlier time point, the lupus-resistant B6.129-*Sle16Sle18* bi-congenics showed comparable percentages of activated ($CD69^+$) lymphocytes (Table I and Figure 3). Consistent with the increase observed in T cell activation status, the $CD4^+$ T cells in aged B6.129-*Sle16* mice were skewed towards an activated memory phenotype with an increased percentage of $CD4^+CD25^-CD44^{high}$ T cells (50.19±1.78 *vs* 33.4±1.49 in B6 mice; $p<0.001$) and a corresponding decrease in the percentage of naïve ($CD62L^+$) T cells

compared to the B6 controls (28.76 % ± 2.23 vs 50.03 ± 2.03 in B6 mice, $p<0.01$, Kruskal-Wallis test with Dunn's multiple comparison test) (Table I). Interestingly, whilst the increase in the memory T cells was comparable between the lupus-prone and the lupus-resistant strains (50.19 ± 1.78 *vs* 48.46 ± 1.86; $p>0.05$), the decrease in the percentage of T cells expressing a naïve phenotype was not observed in the B6.129-*Sle16Sle18* mice (41.27% ± 2.43 *vs* 50.03 ± 2.03 in B6 mice) (Table I and Figure 3).

A more detailed examination of the splenic B cell populations revealed that the B6.129-*Sle16* animals had a small but significant decrease in the percentage of $CD19^+$ B cells, accompanied by a reduction in the MZ B cell population and an increase in the follicular B cells (Table I). We also investigated the percentage of splenic $CD5^+$ $B1^a$ cells and found that this was decreased in the B6.129-*Sle16* mice, a defect that was not present in the B6.129-*Sle16Sle18* bi-congenic mice (Table I and Figure 3). The percentage of plasma cells in the B6.129-*Sle16* animals was markedly augmented compared to the B6 controls and this increase, but to a much lesser degree, was also observed in the B6.129-*Sle16Sle18* bi-congenic mice (Table I).

To substantiate the observations made by flow cytometry, we performed histological analysis of splenic sections in 12 month old mice. In the spleens from the B6.129-*Sle16Sle18* bi-congenic animals we detected a remarkably reduced number of germinal centers compared with the B6.129-*Sle16* mice (Figure 4). These findings indicate that the 129-*Sle18* locus was able to suppress the formation of germinal centers.

Impact of Sle18 on B and T cells

To begin to identify the cellular components contributing to the protection from autoimmunity in B6.129-*Sle16Sle18* mice, we then performed *in vitro* experiments to assess B and T cells responses. We found no differences in the proliferation or immunoglobulin production from splenocytes after stimulation with anti-CD40 or anti-IgM Abs or LPS (data not shown). However, we did observe an increased proliferation of naïve T cells from young B6.129-*Sle16* mice when stimulated *in vitro* with anti-CD3 or PHA and this was accompanied by an enhanced production of IL-2 (Figure 5). The presence of the 129-*Sle18* locus in the double congenic mice restrained the proliferation of the T cells to levels equivalent to those present in the B6 control mice, indicating that the *Sle18* lupus suppressor locus may operate by controlling the proliferative response of naïve T cells.

Surprised by the observed expansion of $FoxP3^+$ T cells in the congenic strains, we then compared the functional competency of the Tregs using an *in vitro* suppressor assay previously described (11). $CD4^+$ T cells were purified from 129.B6-*Sle16Sle18*, 129.B6-*Sle16* and B6 mice and further separated into $CD25^+$ (Treg) and $CD25^-$ Tresp) populations. The freshly isolated Tregs were added to cultures containing a fixed number of Tresp cells at the indicated Treg/ Tresp ratios. The cultures were stimulated with beads coated with anti-CD3 and anti-CD28 Abs and proliferation responses were determined (Figure 6). To compare the suppressive function of the 129.B6-*Sle16Sle18* and 129.B6-*Sle16* Tregs with that of B6 Tregs, we used the same responder T cells (B6 Tresp) (Figure 6A). As previous reports demonstrated that responder T cells from lupus-prone mice have a decreased susceptibility to suppression by Tregs (11), we performed experiments to compare the sensitivity of the different Tresp cells to suppression mediated by the same B6 Treg cells (Figure 6B). Furthermore, we carried out cross-over experiments, in which the suppressive ability of Tregs from 129.B6-*Sle16* or B6 mice to suppress the proliferation of 129.B6-*Sle16* responder T cells was interrogated (Figure 6C). Similarly, the response of Tresp cells from 129.B6-*Sle16* or B6 mice to Tregs from 129.B6-*Sle16* was compared (Figure 6D). These experiments demonstrated that the 129.B6-*Sle16* and 129.B6-*Sle16Sle18* Tregs were fully competent in suppressing B6 Tresp proliferation (Figure 6) in a dose-dependent manner. In

addition, Tresp from 129.B6-*Sle16* and 129.B6*Sle16Sle18* mice were similarly suppressible by B6 or 129.B6-*Sle16* Tregs, indicating no reduced sensitivity to suppression in the congenic animals. Similar results were obtained when suppressor assays using CFSE-labelled responder T cells were performed (data not shown).

Immune responses to TD and TI antigens

We next investigated whether the presence of the *Sle* loci (*Sle16* and *Sle18*) could alter the immune responses to exogenous antigens. We administered a T-dependent (NP-chicken gammaglobulin) and a T-independent (Pneumovax II) antigen to cohorts of age and sex-matched B6, B6.129-*Sle16*, B6.129-*Sle18* and B6.129-*Sle16Sle18* mice. The congenic strains did not substantially differ from the controls in the levels of NP-specific IgG Abs measured at different time points after primary and secondary immunisations. Likewise, anti-NP IgG subclass titres did not differ amongst the congenic cohorts, suggesting a normal class switching process in the congenic mice (Figure 7A). When we assessed the TI immune response, we observed that the strains carrying the *Sle16* locus showed a trend towards higher IgG3 anti-polysaccharide levels, but the values never reached statistical significance at any of the time points analysed. Interestingly, the non-lupus prone strain B6.129-*Sle18* displayed a strong IgM anti-polysaccharide response (day 14: B6.129-*Sle18* 1161 ± 208.8 U/ml *vs* B6.129-*Sle16* 326.8 ± 42.71; $p<0.01$, Kruskal-Wallis test with Dunn's multiple comparison test), but IgG3 titres similar to those detected in the other strains (Figure 7 B).

Discussion

The congenic dissection approach allows identification and analysis of chromosome loci modulating autoimmunity in mice in an effort to determine the underlying genes and the human homologues. This manuscript extends our previous work characterising the suppression of autoimmunity mediated by a novel 129 suppressor locus mapped on chromosome 3. This locus, named 129-*Sle18*, encompasses the central region of chromosome 3 spanning from 71.4 to 129.8 Mb and was able to confer lupus resistance when transferred onto a lupus-prone congenic line, the B6.129-*Sle16* strain (8). The 129-*Sle18*-mediated protection, measured as absence of autoantibodies, was particularly effective in homozygous mice, although the heterozygous 129-*Sle18* allele also resulted in partial protection (Figure 2 and data not shown). These results suggest that the 129-*Sle18* suppressor effect is additive and most likely due to gain of function. In addition, the presence of the 129-*Sle18* locus did not alter the antibody responses to exogenous antigens (TD and TI antigens), indicating that in our model different pathways are used by foreign and self-antigens.

Previous studies on different mouse strains have identified genomic regions with an epistatic "suppressive" effect on disease susceptibility regions or on the phenotype of gene-targeted mice. More specifically, from the genetic dissection of bi and triple congenic models carrying the NZW SLE susceptibility loci *Sle1*, *Sle2* and *Sle3,* four suppressor regions have been characterised. These NZW loci, named SLE suppressors (*Sles*) 1 to 4, have been mapped to chromosome 17, 4, 3 and 9 respectively, and their presence have been shown to abrogate, to a different degree, both the humoral autoimmunity and the nephritis developed by the lupus-prone B6.*Sle* congenic strains (3, 4). Of particular relevance for the data presented in this report is *Sles3* that peaks at 78.6 Mb on chromosome 3 (3) and thus partially overlays with the centromeric end of the 129-*Sle18* allele. Two other suppressive loci have been mapped on chromosome 3: one in the BXSB/long-lived recombinant inbred strain and one in the MRL/*lpr* model (12, 13). Thus suppressor loci in different strains have been mapped to this chromosomal location indicating that at least some of the molecular mechanisms underlying the lupus-resistance may be shared. In this context it is worth mentioning that, though our linkage analysis in (129 × B6)F2 mice failed to identify a strong

Europe PMC Funders Author Manuscripts

lupus modifier locus on chromosome 17 (6, 7), the 129-allele of *Sles1* has been shown to complement the NZW *Sles1* allele in preventing the development of autoimmune features (5). Therefore, it appears that the 129 mice may harbour several *Sle* suppressor loci most likely operating at different molecular levels.

Lupus modifiers act at key steps in the disease pathogenesis and thus their characterisation can be very informative. For example, Wakeland *et al* elegantly demonstrated that the introgression of *Sles1* onto the B6.*Sle1yaa* model, carrying the TLR7 translocation and developing a severe lupus disease, inhibited the phenotype without suppressing the TLR7 hyper-responsiveness linked to the *yaa* locus (14). A lupus-suppressor BALB/c locus, named *sbb2*^{a} and located on chromosome 12, has been shown to reduce the autoimmune pathology of the B6.*Fc*γ*R2B*$^{-/-}$ model. The authors demonstrated that the *sbb2*^{a} locus effect is likely to be B cell extrinsic, probably T cell dependent, and to act *in trans* affecting the IgG2-production by B cells (15). These findings, in agreement with observations in other models (16-18), support the hypothesis that T cells play a critical role in the development of autoimmunity thanks to their physiological function in shaping B cell activation, changing the cytokine milieu and causing tissue damage (19). In our lupus model, the 129-*Sle18* locus affected the autoantibody production driven by the *Sle16* locus apparently without abrogating the development of activated T and B cell populations or altering the number of memory T cells in the spleen. However, the lupus-resistant strain (B6.129-*Sle16Sle18*) had an equivalent percentage of naïve CD62L^{+} T cells to the control mice, suggesting a similar threshold for T activation. This was further supported by the observation *in vitro* that T cells from young B6.129-*Sle16Sle18* mice showed a proliferative response to anti-CD3 Ab stimulation comparable to the B6 mice and significantly less to that observed in the lupus-prone B6.129-*Sle16* strain. These findings suggest that in B6.129-*Sle16Sle18* animals the activated status of T and B cells is not sufficient to drive the lupus phenotype and that the 129-*Sle18* locus may act downstream of these activated molecular pathways. Consistent with this hypothesis, we found a markedly decreased number of germinal centers in the B6.129-*Sle16Sle18* animals compared to the B6.129-*Sle16* strain.

Lupus is well established as a polygenic disease that involves multiple molecular and cellular processes. Therefore it is not surprising that lupus resistance may also be multifactorial. The lupus-prone B6.129-*Sle16* strain displayed splenic B cell abnormalities, as indicated by the contraction of the MZ B cell compartment, already present in young pre-disease animals, and the reduction in the percentage of B1a cells. Both these two B-cell compartments have long been implicated in lupus autoimmunity (20-22) and notably they were restored to normal values by the 129-*Sle18* locus. Similarly, in the lupus resistant TAN mouse, a recombinant strain model bearing a combination of the same *Sle1*, *Sle2* and *Sle3* susceptibility loci together with the *Sles3* NZW suppressor locus, the lupus resistance was found to be associated with an accumulation of splenic B1a cells and an enlargement of the marginal zone B cell compartment (23). Given that the 129-*Sle18* locus partially overlaps with the *Sles3* these data together indicate that some of the underlying mechanisms in these two models might be shared.

MZ B cells are not only the major responders to T-independent antigens but they have been shown to respond more rapidly than follicular B cells to T-dependent antigens and to be more potent T-cell activators (24). Thus, to gain insight into the immune response competence of the congenic strains we challenged the animals with a T-independent and a T-dependent antigen. The congenic lines did not differ from the wild type mice in their antibody responses in either of two immunisation protocols. These data appear to contradict previous observations in B6.*Sle* models, in which blunted antibody responses have been described (25). However, hyper-responsiveness to exogenous antigens have also been

reported in lupus models (26) and these discrepancies may be related to differences in the immunisation protocols applied as well as diverse genetic backgrounds.

Both the lupus-prone and the resistant mice displayed a marked expansion of the Treg compartment compared to the B6 controls, as shown by the increased percentage of splenic $CD4^+CD25^+FoxP3^+$ T cells. This was an intriguing observation given that previous reports have provided evidence of Treg deficiencies (number and/or function) in lupus mice (11, 27-29). In addition, congenic $CD4^+CD25^{high}$ Treg cells, purified from young mice, were functionally competent and just as potent as the B6 Tregs in suppressing the proliferation of normal responder T cells. Of note, an age-dependent biphasic change of Treg frequency has been described in the MRL/lpr mice, with an early increase followed by a subsequent decline mirroring disease progression (30). Therefore, one could speculate that the observed enlargement of the Treg compartment in our model may just reflect a failed attempt of the immune system to control the autoimmune diathesis. However, Treg expansion was also observed in the non-autoimmune B6.129-*Sle18* strain, indicating that other genetic or environmental factors might have contributed to this phenotype.

In summary, in this report we have described a novel 129 lupus-suppressor locus and provided preliminary insights into the mechanisms by which 129-*Sle18* may control the occurrence of spontaneous autoimmunity driven by *Sle16*. Further characterisation of the lupus resistant B6.129-*Sle16Sle18* strain will lead to a better understanding of the mechanisms involved in autoimmune pathogenesis and to useful insights for the development of strategies towards therapeutic interventions.

Acknowledgments

We thank all of the staff in the animal facility for their technical assistance and Ms L Lawrence for the processing of the histological specimens.

4Abbreviations

SLE	Systemic lupus erythematosus
ANA	antinuclear antibody
AP	alkaline phosphatase
AEU	arbitrary ELISA units
Ab	antibody
GN	glomerulonephritis
PHA	phytohemagglutinin
NP-CGG	4-hydroxy-3-nitrophenylacetyl conjugated to chicken gamma globulin
TD	T-cell dependent
TI	T-cell independent

References

1. Fairhurst AM, Wandstrat AE, Wakeland EK. Systemic lupus erythematosus: multiple immunological phenotypes in a complex genetic disease. Adv Immunol. 2006; 92:1–69. [PubMed: 17145301]
2. Rhodes B, Vyse TJ. The genetics of SLE: an update in the light of genome-wide association studies. Rheumatology (Oxford). 2008; 47:1603–1611. [PubMed: 18611920]

3. Morel L, Tian XH, Croker BP, Wakeland EK. Epistatic modifiers of autoimmunity in a murine model of lupus nephritis. Immunity. 1999; 11:131–139. [PubMed: 10485648]
4. Morel L, Croker BP, Blenman KR, Mohan C, Huang G, Gilkeson G, Wakeland E. Genetic reconstitution of systemic lupus erythematosus immunopathology with polycongenic murine strains. PNAS. 2000; 97:6670–6675. [PubMed: 10841565]
5. Subramanian S, Yim YS, Liu K, Tus K, Zhou XJ, Wakeland EK. Epistatic suppression of systemic lupus erythematosus: fine mapping of Sles1 to less than 1 mb. J Immunol. 2005; 175:1062–1072. [PubMed: 16002707]
6. Bygrave AE, Rose KL, Cortes-Hernandez J, Warren J, Rigby RJ, Cook HT, Walport MJ, Vyse TJ, Botto M. Spontaneous autoimmunity in 129 and C57BL/6 mice-implications for autoimmunity described in gene-targeted mice. PLoS Biol. 2004; 2:E243. [PubMed: 15314659]
7. Heidari Y, Bygrave AE, Rigby RJ, Rose KL, Walport MJ, Cook HT, Vyse TJ, Botto M. Identification of chromosome intervals from 129 and C57BL/6 mouse strains linked to the development of systemic lupus erythematosus. Genes Immun. 2006; 7:592–599. [PubMed: 16943797]
8. Carlucci F, Cortes-Hernandez J, Fossati-Jimack L, Bygrave AE, Walport MJ, Vyse TJ, Cook HT, Botto M. Genetic dissection of spontaneous autoimmunity driven by 129-derived chromosome 1 Loci when expressed on C57BL/6 mice. J Immunol. 2007; 178:2352–2360. [PubMed: 17277141]
9. Liu K, Mohan C. What do mouse models teach us about human SLE? Clin Immunol. 2006; 119:123–130. [PubMed: 16517211]
10. Heidari Y, Fossati-Jimack L, Carlucci F, Walport MJ, Cook HT, Botto M. A lupus-susceptibility C57BL/6 locus on chromosome 3 (Sle18) contributes to autoantibody production in 129 mice. Genes Immun. 2009; 10:74–55.
11. Monk CR, Spachidou M, Rovis F, Leung E, Botto M, Lechler RI, Garden OA. MRL/Mp CD4+,CD25− T cells show reduced sensitivity to suppression by CD4+,CD25+ regulatory T cells in vitro: a novel defect of T cell regulation in systemic lupus erythematosus. Arthritis Rheum. 2005; 52:1180–1184. [PubMed: 15818683]
12. Haywood ME, Gabriel L, Rose SJ, Rogers NJ, Izui S, Morley BJ. BXSB/long-lived is a recombinant inbred strain containing powerful disease suppressor loci. J Immunol. 2007; 179:2428–2434. [PubMed: 17675504]
13. Wang Y, Nose M, Kamoto T, Nishimura M, Hiai H. Host modifier genes affect mouse autoimmunity induced by the lpr gene. Am J Pathol. 1997; 151:1791–1798. [PubMed: 9403730]
14. Subramanian S, Tus K, Li QZ, Wang A, Tian XH, Zhou J, Liang C, Bartov G, McDaniel LD, Zhou XJ, Schultz RA, Wakeland EK. A Tlr7 translocation accelerates systemic autoimmunity in murine lupus. Proc Natl Acad Sci U S A. 2006; 103:9970–9975. [PubMed: 16777955]
15. Tarasenko T, Kole HK, Bolland S. A lupus-suppressor BALB/c locus restricts IgG2 autoantibodies without altering intrinsic B cell-tolerance mechanisms. J Immunol. 2008; 180:3807–3814. [PubMed: 18322187]
16. Mohan C, Yu Y, Morel L, Yang P, Wakeland EK. Genetic dissection of Sle pathogenesis: Sle3 on murine chromosome 7 impacts T cell activation, differentiation, and cell death. J Immunol. 1999; 162:6492–6502. [PubMed: 10352264]
17. Vratsanos GS, Jung S, Park YM, Craft J. CD4+ T cells from lupus-prone mice are hyperresponsive to T cell receptor engagement with low and high affinity peptide antigens: a model to explain spontaneous T cell activation in lupus. J Exp Med. 2001; 193:329–337. [PubMed: 11157053]
18. Linterman MA, Rigby RJ, Wong RK, Yu D, Brink R, Cannons JL, Schwartzberg PL, Cook MC, Walters GD, Vinuesa CG. Follicular helper T cells are required for systemic autoimmunity. J Exp Med. 2009; 206:561–576. [PubMed: 19221396]
19. Hoffman RW. T cells in the pathogenesis of systemic lupus erythematosus. Clin Immunol. 2004; 113:4–13. [PubMed: 15380523]
20. Grimaldi CM, Michael DJ, Diamond B. Cutting edge: expansion and activation of a population of autoreactive marginal zone B cells in a model of estrogen-induced lupus. J Immunol. 2001; 167:1886–1890. [PubMed: 11489967]
21. Li Y, Li H, Weigert M. Autoreactive B cells in the marginal zone that express dual receptors. J Exp Med. 2002; 195:181–188. [PubMed: 11805145]

22. Wither JE, Loh C, Lajoie G, Heinrichs S, Cai YC, Bonventi G, MacLeod R. Colocalization of expansion of the splenic marginal zone population with abnormal B cell activation and autoantibody production in B6 mice with an introgressed New Zealand Black chromosome 13 interval. J Immunol. 2005; 175:4309–4319. [PubMed: 16177071]
23. Duan B, Croker BP, Morel L. Lupus resistance is associated with marginal zone abnormalities in an NZM murine model. Lab Invest. 2007; 87:14–28. [PubMed: 17170739]
24. Attanavanich K, Kearney JF. Marginal zone, but not follicular B cells, are potent activators of naive CD4 T cells. J Immunol. 2004; 172:803–811. [PubMed: 14707050]
25. Niu H, Sobel ES, Morel L. Defective B-cell response to T-dependent immunization in lupus-prone mice. Eur J Immunol. 2008; 38:3028–3040. [PubMed: 18924209]
26. Park CL, Balderas RS, Fieser TM, Slack JH, Prud'Homme GJ, Dixon FJ, Theofilopoulos AN. Isotypic profiles and other fine characteristics of immune responses to exogenous thymus-dependent and - independent antigens by mice with lupus syndromes. J Immunol. 1983; 130:2161–2167. [PubMed: 6339623]
27. Chen Y, Cuda C, Morel L. Genetic determination of T cell help in loss of tolerance to nuclear antigens. J Immunol. 2005; 174:7692–7702. [PubMed: 15944270]
28. Cuda CM, Wan S, Sobel ES, Croker BP, Morel L. Murine lupus susceptibility locus Sle1a controls regulatory T cell number and function through multiple mechanisms. J Immunol. 2007; 179:7439–7447. [PubMed: 18025188]
29. Abe J, Ueha S, Suzuki J, Tokano Y, Matsushima K, Ishikawa S. Increased Foxp3(+) CD4(+) regulatory T cells with intact suppressive activity but altered cellular localization in murine lupus. Am J Pathol. 2008; 173:1682–1692. [PubMed: 19008373]
30. Yang CH, Tian L, Ling GS, Trendell-Smith NJ, Ma L, Lo CK, Stott DI, Liew FY, Huang FP. Immunological mechanisms and clinical implications of regulatory T cell deficiency in a systemic autoimmune disorder: roles of IL-2 versus IL-15. Eur J Immunol. 2008; 38:1664–1676. [PubMed: 18465774]

Europe PMC Funders Author Manuscripts

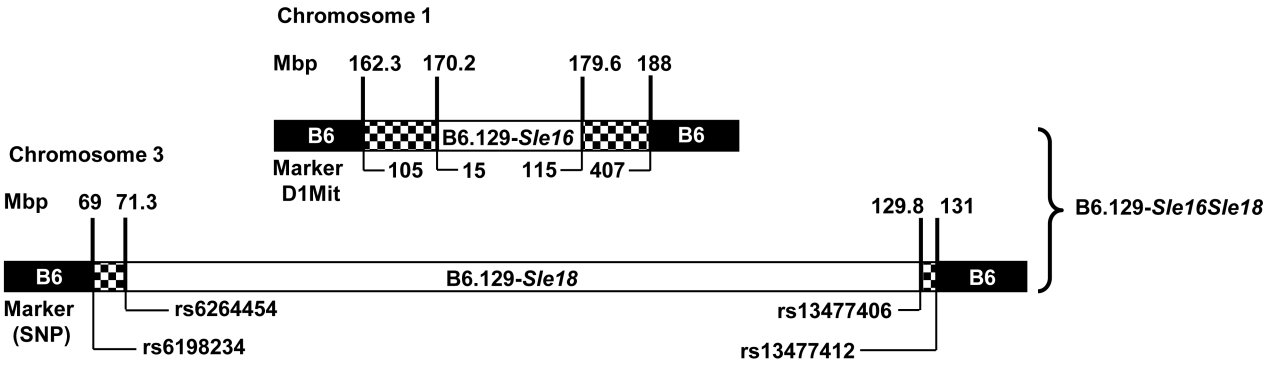

Figure 1.

Genetic map of congenic mice bearing the *Sle16* and *Sle18* regions. Loci position (shown in Mbp) has been defined by microsatellite and SNP genotyping (list on request). White = 129 genome, black = B6 genome, hatched = recombination regions.

Europe PMC Funders Author Manuscripts

Europe PMC Funders Author Manuscripts

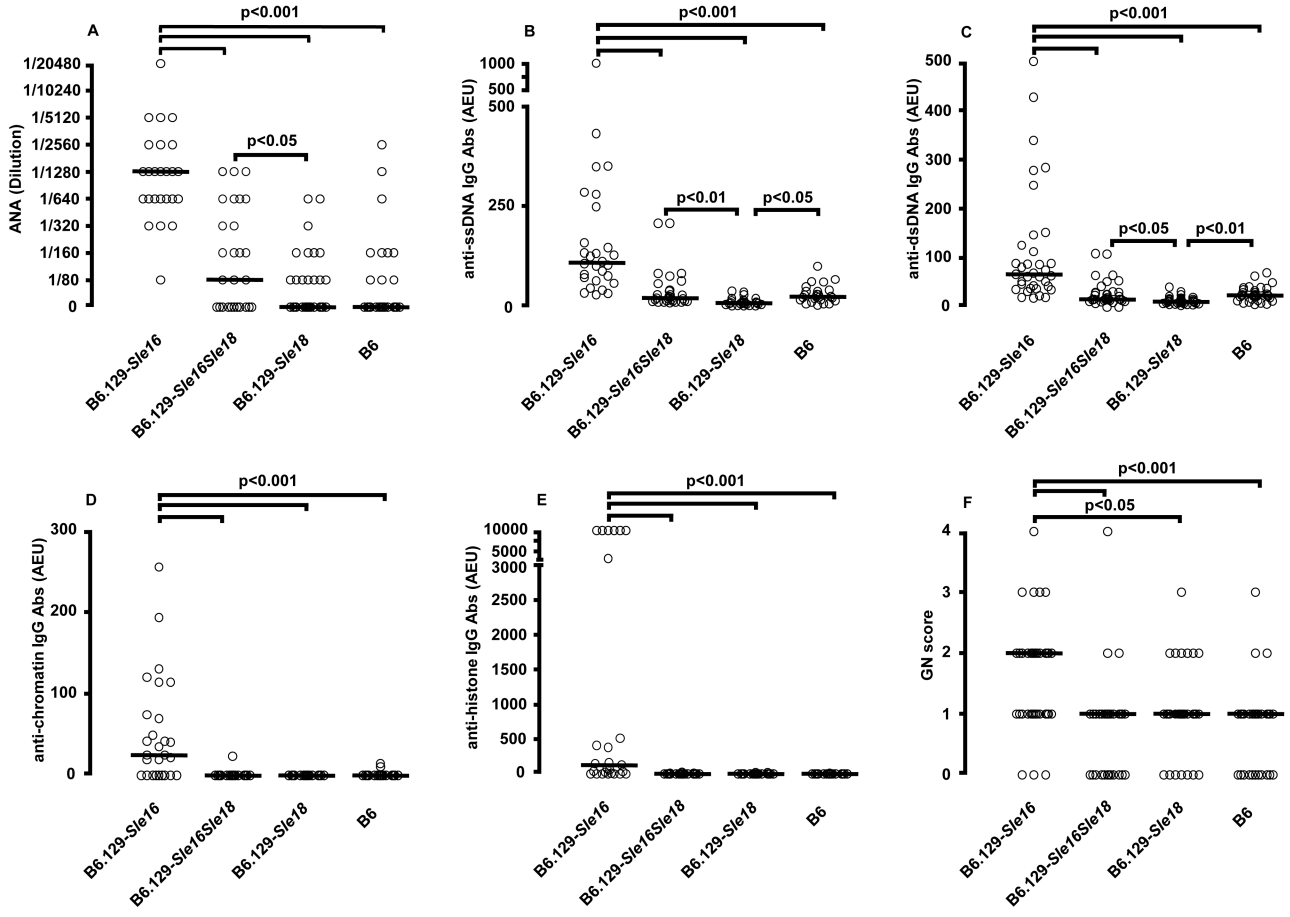

Figure 2.

Serological and histological profiles at one year of age**.** Each symbol represents one mouse. A) ANA titers. Serum samples were screened at 1/80 and positives titrated to endpoint, B) anti-ssDNA Ab, C) anti-dsDNA Ab, D) anti-chromatin Ab and E) anti-histone Ab levels in the B6.129 congenic lines are shown. The antibody levels are expressed in arbitrary ELISA units related to a standard positive sample. F) Glomerulonephritis graded from 0 to 4 as described in Materials and Methods. Horizontal bars indicate median. The non-parametric Kruskal-Wallis test with Dunn's multiple comparison test was applied throughout with differences being considered significant for p values <0.05. AEU = arbitrary ELISA unit

Europe PMC Funders Author Manuscripts

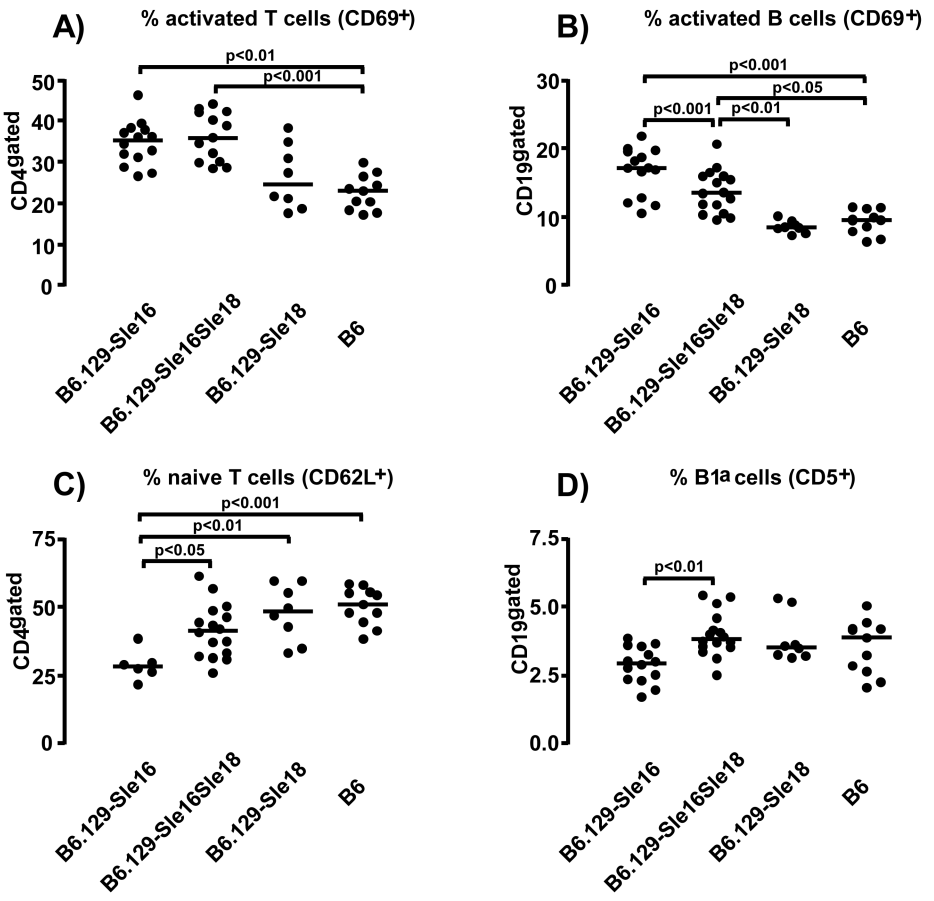

Figure 3.

Lymphocyte population distribution in the spleens of 12 month-old mice. The percentage of activated $CD69^+$ T cell (A) and B cells (B) are shown. Graphs illustrating the proportion of (C) naive $CD4^+$ T cells ($CD62L^+$) and (D) of B1a cells ($CD19^+CD5^+$) are presented. For each panel all significant differences, determined by the Kruskal-Wallis test with Dunn's multiple comparison test, are indicated. Each symbol represents one mouse and the horizontal lines designate means.

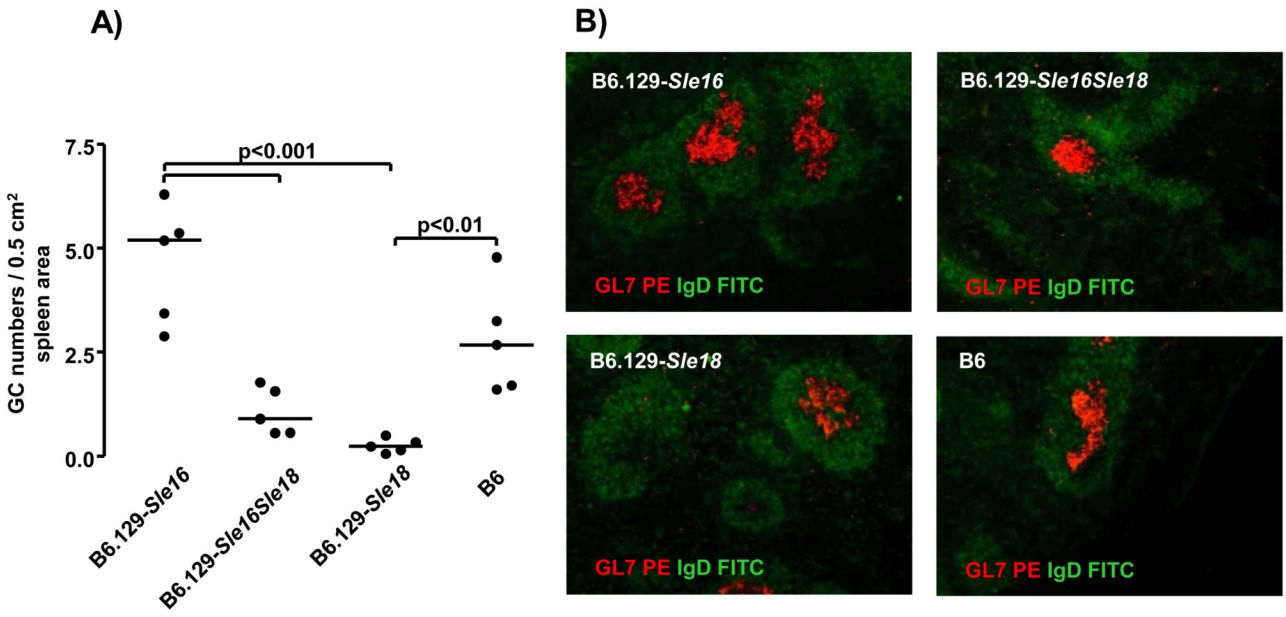

Figure 4.

Germinal center quantification by immunoflourescence in 12 month old mice. A) Germinal centre number/0.5 cm^2 spleen area in the three congenic lines and wild-type control. Each symbol represents one mouse; Bonferroni's multiple comparison test was applied throughout with differences being considered significant for p values <0.05. GC = germinal centre. B) Examples of spleen sections showing GC (anti-GL7, red) and follicular zone B cells (anti-IgD, green) in congenic and wild-type mice.

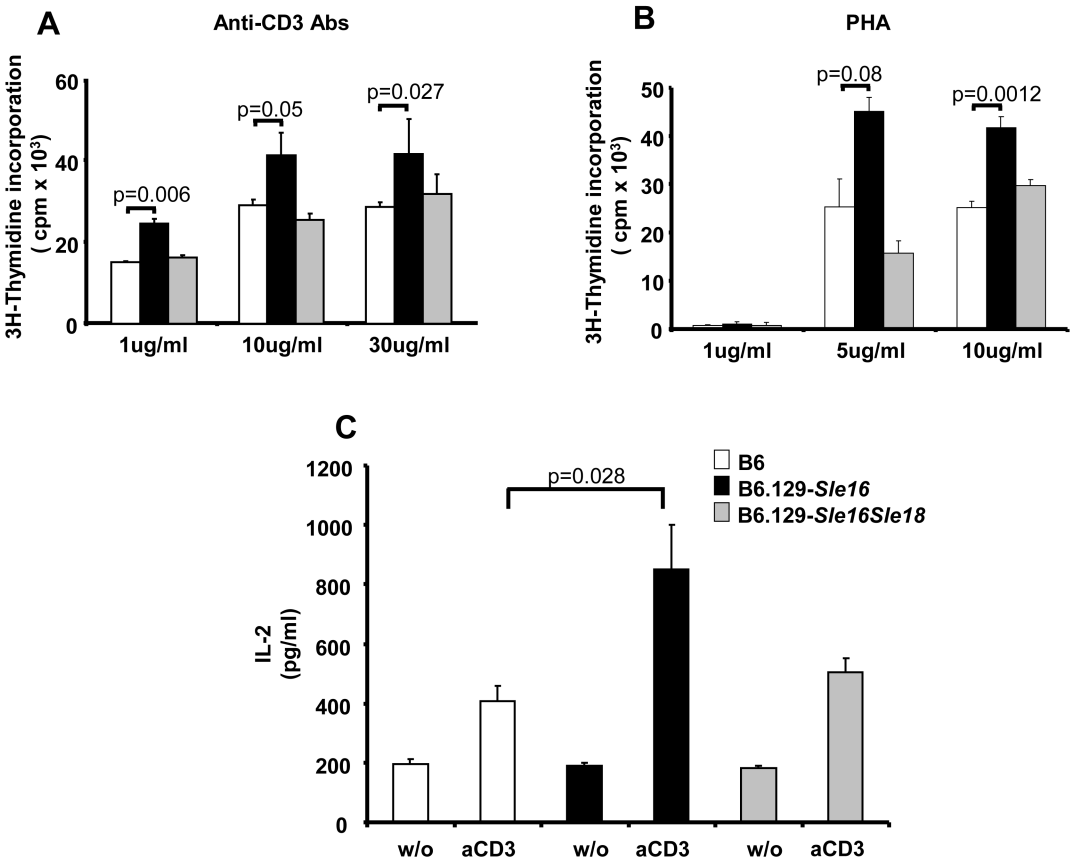

Figure 5.

Stimulation of naïve T cells. $CD4^{+}CD25^{-}$ naïve T cells were purified from 2-3 month old mice (for details see Materials and Methods). Cells were cultured alone (w/o) or in the presence of plated-bound anti-CD3 antibody (aCD3) (A) or PHA (B) at different concentrations. Cell proliferation was determined by thymidine incorporation after 3 days of stimulation (^{3}H thymidine added for the last 16hours). C) Serum IL-2 levels were determined in the culture supernatants after stimulation with plated-bound anti-CD3 Ab (1μg/ml) using ELISA. Shown are data (mean ± SD) representative of 3 independent experiments. The data were analysed by two-tailed Student's t-test. The genotypes of the mice are shown.

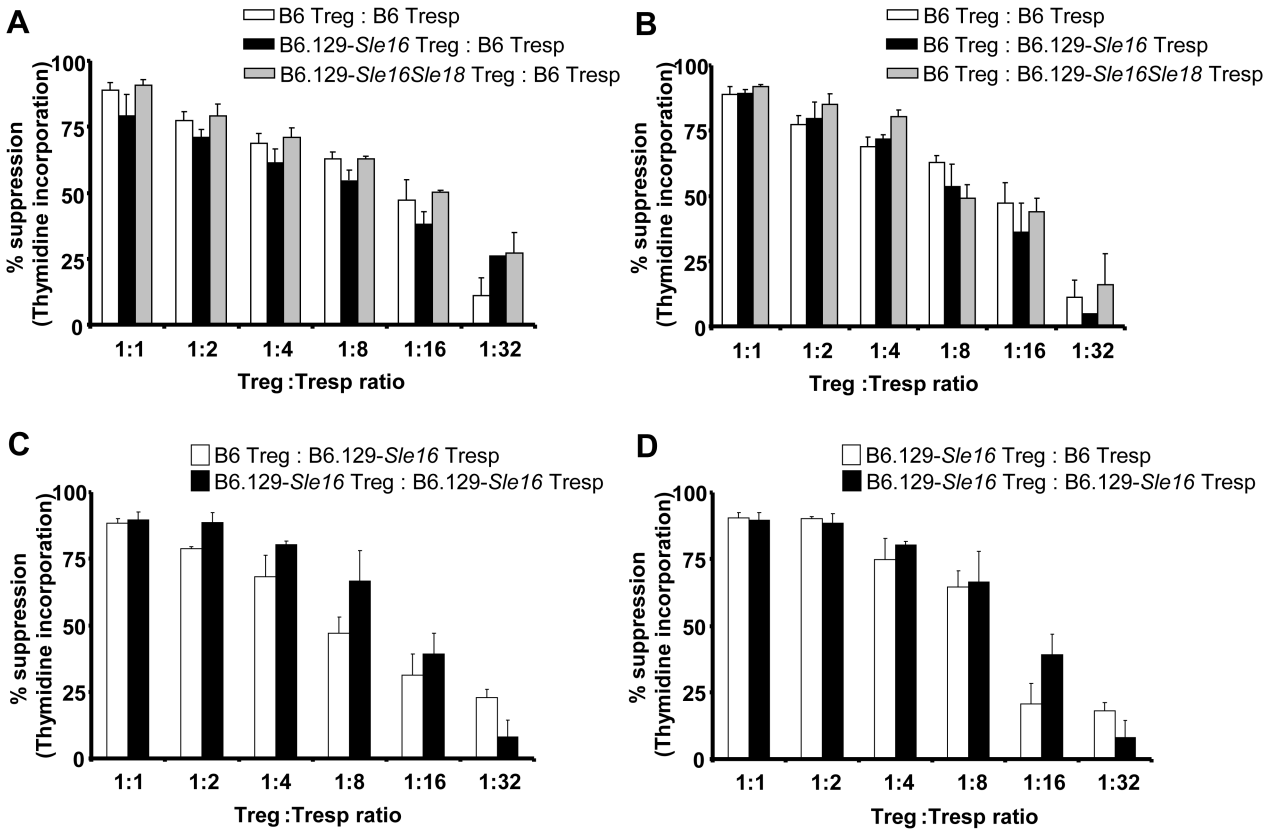

Figure 6.

Suppressor T cell assays in 2-3 month old animals. Purified $CD4^+CD25^+$ regulatory T cells were cultured with $CD4^+CD25^-$ responder T cells (at the indicated Treg:Tresp ratios) in the presence of beads coated with anti-CD3 and anti-CD28 mAb (for details see Materials and Methods). Inhibition of $CD4^+CD25^-$ T cell proliferation relative to a 0:1 Treg:Tresp ratio was measured by $[^3H]$thymidine incorporation. A) The suppressive function of Tregs from B6.129-*Sle16Sle18* and B6.129–*Sle16* mice was compared with that of B6 Treg cells. B) The sensitivity to suppression of responder T cells from B6.129-*Sle16Sle18* and B6.129–*Sle16* mice was compared with that of B6 Tresp. C) The suppressive activity of Tregs from B6.129–*Sle16* or B6 mice was tested using Tresp from B6.129–*Sle16* mice. D) The susceptibility to suppression by B6.129–*Sle16* Tregs of Tresp from B6.129–*Sle16* or B6 mice was compared. Results shown (mean ± SD) are representative of three independent experiments and were performed on 2-3 month old mice.

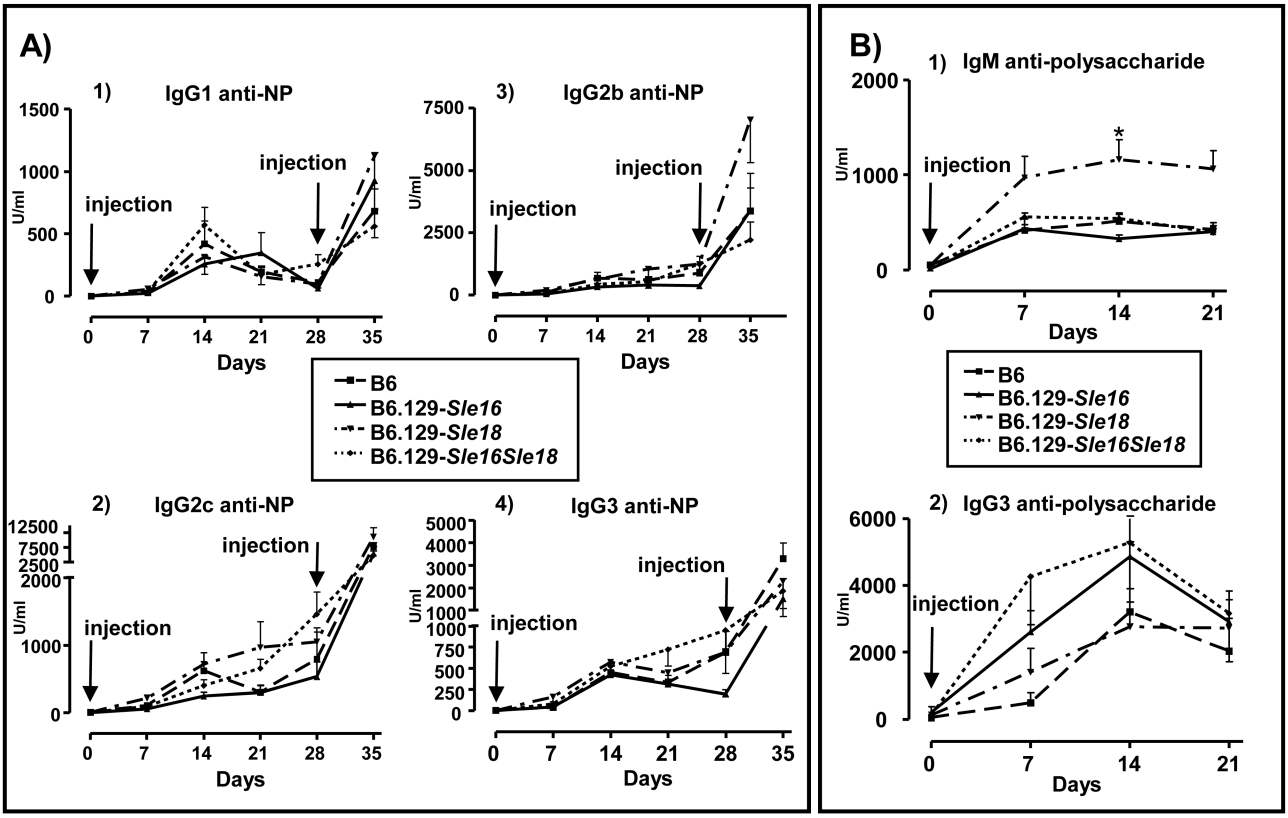

Figure 7.

Immune response to exogenous antigens. A) T-dependent immunization. All cohorts showed equivalent responses to immunisation to NP-CGG administrated subcutaneously with complete Freund's adjuvant, as determined by ELISA measurements of NP-specific IgG Abs. B) T-independent immunization. Levels of IgM and IgG3 anti-polysaccharide Abs in serum diluted 1/1000 (IgM) and 1/100 (IgG3). Each symbol represents the mean (± SEM) of the values from at least 5 mice per strain per time point. Time points are indicated in days after the primary immunisation. Arrows indicate time of injection. * indicate when statistical difference was reached at a given time point. Kruskal-Wallis test with Dunn's multiple comparison test was applied throughout with differences being considered significant for p values <0.05. NP-CGG=4-hydroxy-3-nitrophenylacetyl conjugated to chicken gamma globulin.

Europe PMC Funders Author Manuscripts

Europe PMC Funders Author Manuscripts

J Immunol. Author manuscript; available in PMC 2013 July 02.

Table I

Flow cytometric analysis of splenic cell populations at 6 and 12 months of age.

Cell population	FACS staining	6 months				12 months			
		Sle16 ***No= 7***	***Sle16Sle18*** ***No= 8***	***Sle18*** ***No= 8***	***B6*** ***No= 7***	***Sle16*** ***No= 14***	***Sle16Sle18*** ***No= 12***	***Sle18*** ***No= 8***	***B6*** ***No= 11***
Cells (10^6 /ml)		62.18 ± 4.47$	38.49 ± 5.67	39.99 ± 5.02	43.09 ± 3.13	92.57 ± 6.99***, $$, †	52.33 ± 2.77	50 ± 2.93	38.94 ± 4.77
% B cells (No ×10^6)	$CD19^+$	44.97 ± 2.2 (27.34 ± 2.48$)	44.15 ± 1.36 (16.99 ± 2.54)	45.92 ± 2.46 (18.29 ± 2.23)	37.49 ± 1.65 (16.37 ± 1.76)	42.29 ± 1.18*, $$$ (38.8 ± 2.73***, †)	54.46 ± 1.18 (28.94 ± 1.95)	46.97 ± 2.01 (23.5 ± 1.75)	50.28 ± 2.01 (19.58 ± 2.56)
% T cells (No ×10^6)	$CD19^-$, $CD5^+$	40.09 ± 1.57 (25.49 ± 1.85)	43.87 ± 1.33 (16.96 ± 2.69)	42.16 ± 2.76 (17.14 ± 2.91)	45.72 ± 2 (19.62 ± 1.46)	31.71 ± 1.48 (29.33 ± 2.71**, $$, †)	28.94 ± 1.69* (15.34 ± 1.23)	29.67 ± 1.71 (14.89 ± 1.25)	36.22 ± 1.85 (13.96 ± 1.77)
% Plasma cells (No ×10^6)	$CD19^-$, $CD90^-$,$CD138^+$	0.69 ± 0.26 (0.42 ± 0.16)	0.56 ± 0.11 (0.23 ± 0.05)	0.56 ± 0.09 (0.2 ± 0.02)	0.55 ± 0.03 (0.23 ± 0.01)	2.05 ± 0.19***, ††† (1.94 ± 0.28***, $, †††)	1.35 ± 0.11* (0.75 ± 0.09**)	0.72 ± 0.07 (0.36 ± 0.04)	0.62 ± 0.09 (0.21 ± 0.02)
% MZ B cells (No ×10^6)	$CD19^{gated}CD21^{high}CD23^{low}$	8.9 ± 1.64 (2.61 ± 0.55)	11.02 ± 1.18 (1.99 ± 0.46)	11.99 ± 1.2 (2.12 ± 0.28)	9.2 ± 0.45 (1.51 ± 0.20)	6.25 ± 0.69**, $ (2.4 ± 0.32)	9.11 ± 0.56 (2.66 ± 0.28)	6.87 ± 0.68* (1.59 ± 0.16)	10.78 ± 0.82 (2.21 ± 0.38)
% FZ B cells (No ×10^6)	$CD19^{gated}CD21^{low}CD23^{high}$	63.24 ± 3.73 (17.33 ± 2.68)	63.13 ± 2.42* (10.45 ± 1.28)	62.5 ± 1.18* (11.55 ± 1.57)	73.43 ± 0.84 (12.09 ± 1.39)	69.27 ± 1.37* (26.81 ± 1.86***, ††)	67.13 ± 1.74 (19.13 ± 1.08)	68.09 ± 3.79 (16.13 ± 1.8)	61.4 ± 1.26 (11.95 ± 1.54)
% B1a cells (No ×10^6)	$CD19^{gated}CD5^+$	3.42 ± 0.25 (0.91 ± 0.06$)	2.78 ± 0.25 (0.55 ± 0.06)	3.76 ± 0.28 (0.65 ± 0.05)	3.67 ± 0.16 (0.59 ± 0.05)	2.89 ± 0.17$$ (1.11± 0.1*)	3.98 ± 0.19 (1.19 ± 0.13*)	3.84 ± 0.3 (0.9 ± 0.08)	3.54 ± 0.29 (0.66 ± 0.08)
% activated B cells (No ×10^6)	$CD19^{gated}CD69^+$	10.22 ± 0.88 (2.85 ± 0.19$, ††)	7.96 ± 0.41 (1.36 ± 0.21)	6.95 ± 0.99 (1.22 ± 0.23)	9.14 ± 0.74 (1.44 ± 0.10)	16.61 ± 0.93***, ††† (6.42 ± 0.61***, †††)	13.78 ± 0.77*, ‡‡ (4.02 ± 0.35*, ‡)	8.61 ± 0.31 (2 ± 0.12)	9.33 ± 0.52 (1.86 ± 0.27)
% activated T cells (No ×10^6)	$CD4^{gated}CD69^+$	20.56 ± 2.6** (5.86 ± 0.68*)	19.29 ± 0.87* (3.18 ± 0.41)	18.69 ± 0.97 (3.21 ± 0.58)	12.89 ± 0.78 (2.55 ± 0.28)	34.54 ± 1.41** (10.22 ± 1.11***, $, ††)	35.39 ± 1.8*** (5.5 ± 0.58)	26.34 ± 2.72 (3.79 ± 0.34)	22.65 ± 1.27 (3.14 ± 0.41)
% naïve T cells (No ×10^6)	$CD4^{gated}CD62L^+$	57.84 ± 3.26 (14.6 ± 0.98)	60.37 ± 1.46 (10.55 ± 2.16)	63.37 ± 1.77 (11.11 ± 2.14)	65.52 ± 1.61 (12.94 ± 1.14)	¶28.76 ± 2.23**, †† (8.27 ± 1.17)	41.27 ± 2.43 (6.4 ± 0.65)	47.57 ± 3.6 (7.2 ± 0.96)	50.03 ± 2.03 (7.2 ± 1.08)
% Memory T cells (No ×10^6)	$CD4^{gated}CD44^{high}CD25^-$	28.39 ± 2.5 (7.43 ± 1.11†)	28.51 ± 1.49 (4.59 ± 0.53)	25.74 ± 1.9 (4.11 ± 0.44)	24.04 ± 1.02 (4.67 ± 0.31)	50.19 ± 1.78*** (14.66 ± 1.4***, $, ††)	48.46 ± 1.86*** (7.33 ± 0.58)	41.64 ± 3.3 (6.01 ± 0.45)	33.4 ± 1.49 (4.46 ± 0.43)
% Regulatory T cells (No ×10^6)	$CD4^{gated}CD25^+FoxP3^+$	20.47 ± 1.95** (5.24 ± 0.7**)	17.61 ± 0.97** (2.98 ± 0.4)	16.88 ± 0.81* (2.8 ± 0.37)	10.17 ± 0.3 (2.01 ± 0.2)	27.83 ± 1.51* (8.18 ± 0.92***, $)	27.62 ± 1.11* (4.29 ± 0.43)	Not available	22.59 ± 1.23 (3.03 ± 0.32)

Results are shown as mean ± SEM. P values considered significant when <0.05 according to the Kruskal-Wallis test with Dunn's multiple comparison test. Statistical analysis as follow:

Europe PMC Funders Author Manuscripts

[*] any congenic *vs* B6,

[$] *Sle16 vs Sle16Sle18*,

[†] *Sle16 vs Sle18*;

[‡] *Sle16Sle18 vs Sle18*.

One symbol: <0.05, two symbols: <0.01, three symbols: <0.001.

[¶] CD62L staining was available only for 6 mice. When gated cells are indicated, the percentage refers to the percentage of the gated population. No = number; MZ= marginal zone; FZ: follicular zone.